

Electronic Supplementary Information

Understanding ionic mesophase stabilization by hydration: A solid-state NMR study

Debashis Majhi, Jing Dai, Andrei V. Komolkin, and Sergey V. Dvinskikh*

Table of Contents

S1. Materials and Methods

S2. ^{13}C - ^1H PDLF experiment in static sample

S3. ^{13}C - ^1H APM-CP experiment in spinning sample

S4. ^{13}C - ^{13}C dipolar CP-INADEQUATE experiment at natural isotopic abundance

S5. ^{13}C - ^{15}N dipolar spectroscopy at natural isotopic abundance

S6. Natural abundance deuterium (NAD) NMR

S7. Bond order parameters S_{CH} in the imidazolium ring of the C_{12}mim cation with different anions

S8. ^1H isotropic chemical shifts

S9. Water translational diffusion in $\text{C}_{12}\text{mimBr}\cdot\text{H}_2\text{O}$

S1. Materials and Methods

Ionic mesogenic materials $C_{12}mimCl$ and $C_{12}mimBr$ (1-dodecyl-3-methylimidazolium chloride and bromide, respectively) were purchased from ABCR GmbH, Karlsruhe. Monohydrated samples were prepared by equilibrating for about 12 h in a desiccator with $RH \approx 85\%$, stabilized by a saturated KCl solution. Representative NMR spectra of samples in mesophase are shown in Fig. S1a,b.

Table S1. Water contents and phase transition temperatures

Ionic liquid	H ₂ O mole fraction ^{a)}	$T_{Cr \rightarrow Sm}$, °C	$T_{Iso \rightarrow Sm}$, °C
$C_{12}mimCl$	0.004	36	118
$C_{12}mimCl \cdot H_2O$	0.48	30	154
$C_{12}mimBr$	0.025	40	102
$C_{12}mimBr \cdot H_2O$	0.50	36	129

^{a)} Water content was estimated from 1H NMR spectra in isotropic phase

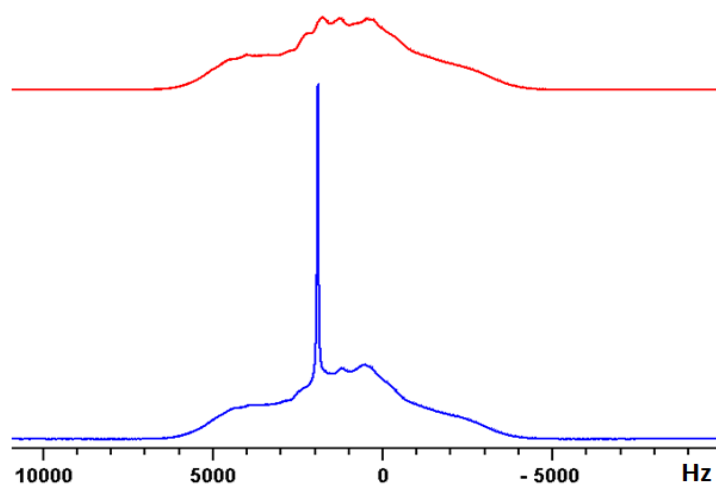


Figure S1a. Proton NMR spectra in smectic A phase of anhydrous (top, 95°C) and monohydrated (bottom, 120°C) $C_{12}mimCl$ salt.

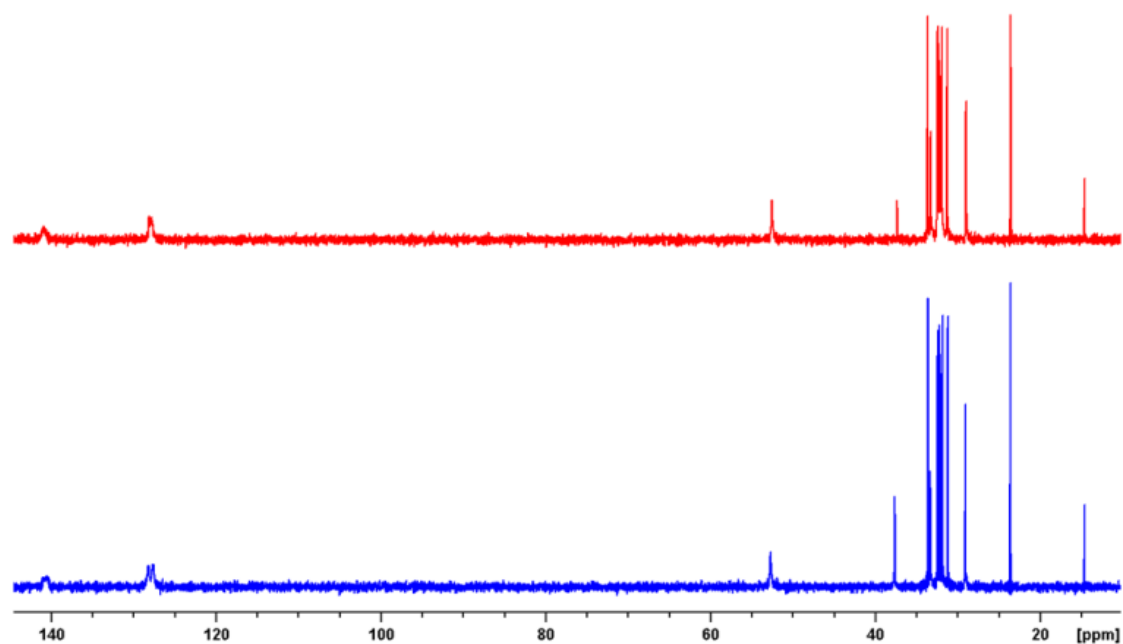


Figure S1b. Carbon-13 cross-polarization (CP) proton-decoupled NMR spectra in the smectic A phase of anhydrous (top, 95°C) and monohydrated (bottom, 120°C) C₁₂mimCl salt. In uniaxial mesophases, the rigid-lattice CSA tensor is averaged into an axially symmetric tensor with principal components δ_{\parallel} and δ_{\perp} , corresponding to LC domains with the director oriented parallel and perpendicular to the magnetic field, respectively, and with isotropic chemical shift $\delta^{\text{iso}} = (\delta_{\parallel}^{LC} + 2\delta_{\perp}^{LC})/3$. In our samples, which exhibit a negative anisotropy of the diamagnetic susceptibility, the director aligns in the plane perpendicular to the magnetic field of the spectrometer. Hence, the observed chemical shifts are determined by the δ_{\perp}^{LC} values.¹

S2. ^{13}C - ^1H PDLF experiment in static sample

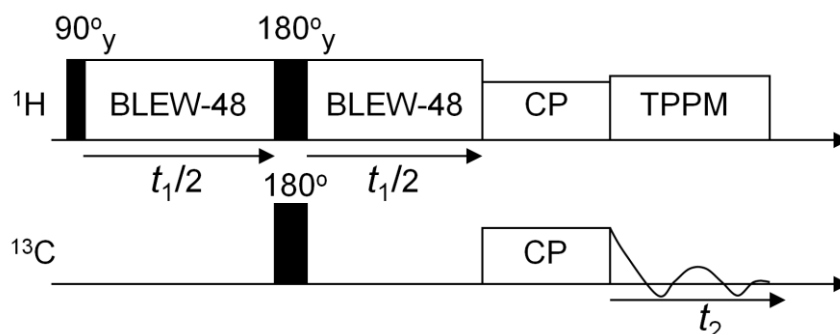


Figure S2a. PDLF pulse sequence to record dipolar ^{13}C - ^1H spectra in static samples. In the indirect time period t_1 of the PDLF experiment,² proton (^1H) magnetization evolves in the presence of the local dipolar fields of rare ^{13}C spins. Application of the proton homonuclear decoupling sequence BLEW-48 scales the heteronuclear couplings d_{CH} with a factor of $k \approx 0.42$.³ A pair of 180° pulses is applied at $t_1/2$ to refocus ^1H chemical shifts while retaining the ^1H - ^{13}C couplings. The proton magnetization is transferred to ^{13}C spins via CP and the carbon signal is detected under TPPM ^1H heteronuclear decoupling.⁴

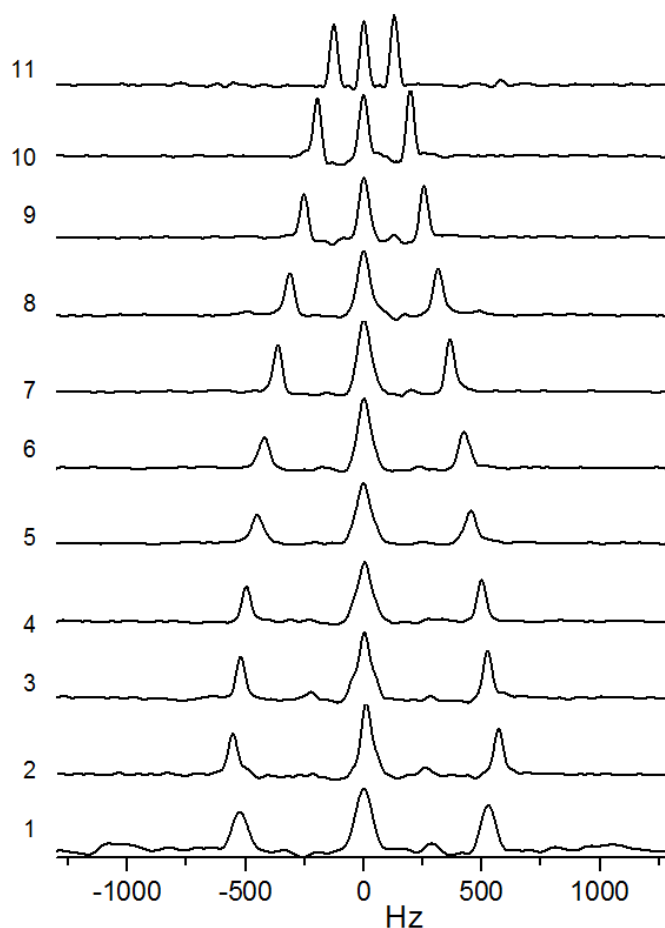


Figure S2b. Cross-sections along dipolar dimension from 2D PDLF spectrum in $\text{C}_{12}\text{mimBr}\cdot\text{H}_2\text{O}$ smectic A phase at 107°C are shown for the alkyl chain carbons.

S3. ^{13}C - ^1H APM-CP experiment in spinning sample

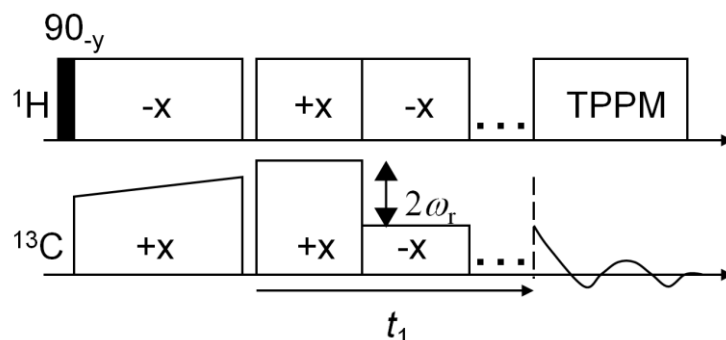


Figure S3a. APM-CP pulse sequence to record dipolar ^{13}C - ^1H spectra in spinning samples.^{5,6} After the CP signal enhancement, the dipolar evolution period is initiated by inverting the phase of the ^1H spin-lock field. The rf fields during t_1 period are phase- and amplitude-modulated to achieve the ^1H - ^{13}C heteronuclear dipolar recoupling. Finally, the ^{13}C signal is detected in the presence of the heteronuclear ^1H decoupling.

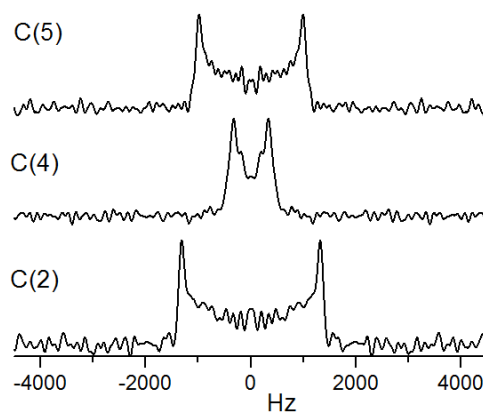


Figure S3b. Cross-sections along dipolar dimension from 2D APM-CP spectrum in $\text{C}_{12}\text{mimCl}$ smectic A phase at 73°C are shown for the imidazolium carbons. Spectra were measured at 5 kHz sample spinning speed and with average recoupling radio-frequency field of $\gamma B_1/2\pi = 28$ kHz.

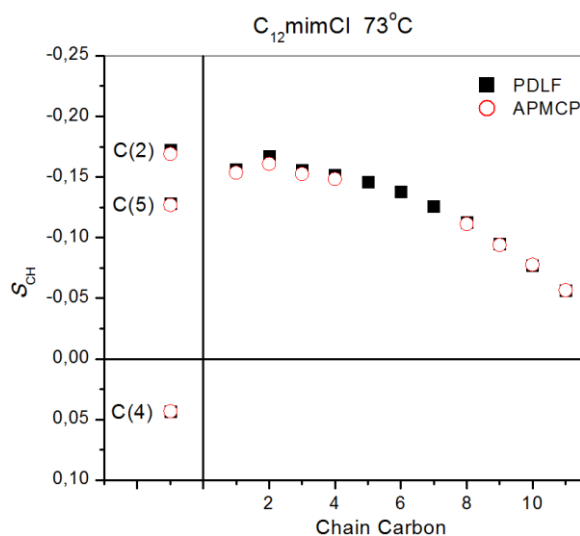


Figure S3c. Comparison of the C-H bond order parameters S_{CH} obtained from PDLF and APM-CP experiments in $\text{C}_{12}\text{mimCl}$ smectic A phase at 73°C . Carbon sites 5–7 of the alkyl chain were not resolved in APM-CP spectrum.

S4. ^{13}C - ^{13}C dipolar CP-INADEQUATE experiment at natural isotopic abundance.

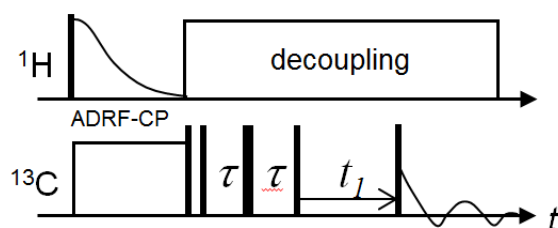


Figure S4a. INADEQUATE pulse sequence⁷ was modified by (i) using ADRF CP for ^{13}C signal enhancement⁸ and (ii) setting the excitation delay τ to generate double quantum (DQ) coherences according to range of dipolar couplings to be measured.⁹

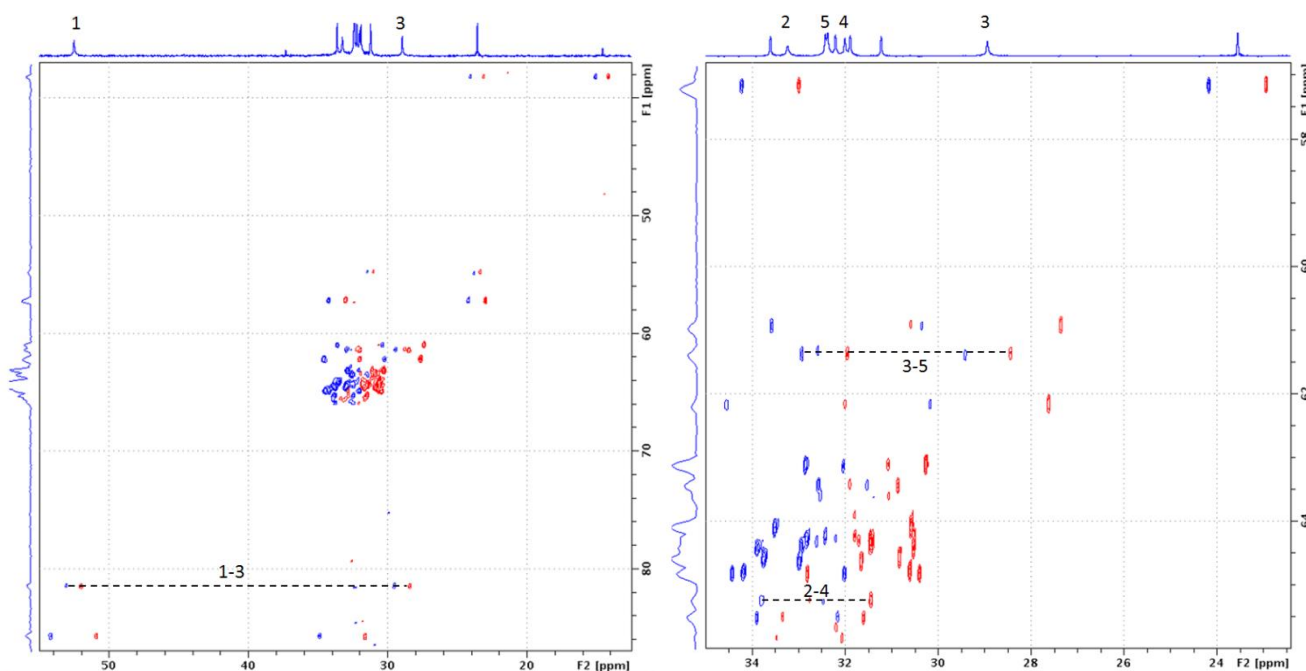


Figure S4b. ^{13}C - ^{13}C INADEQUATE spectra in the smectic A phase of $\text{C}_{12}\text{mimCl}$ at $95\text{ }^\circ\text{C}$. The excitation delay in DQ-filter is set to $\tau = 0.83\text{ ms}$. Correlation peaks between chain carbons 1-3, 2-4, and 3-5 separated by two bonds are indicated by dashed lines. The observed splittings $\Delta\nu$, contributed by the C-C dipolar coupling depend on the frequency difference $\Delta\delta$ between involved spins. When $\Delta\delta$ is small compared to the splitting $\Delta\nu$, the dipolar coupling is given by $d_{\text{CC}} = \Delta\nu/3$, while for the opposite case $d_{\text{CC}} = (\Delta\nu - J)/2$. For intermediate cases, numerical analysis was performed to determine d_{CC} . For carbons separated by two bonds, literature values of the J -coupling are small, within 0-2 Hz range, and were neglected in the analysis.¹⁰

S5. ^{13}C - ^{15}N dipolar spectroscopy at natural isotopic abundance.

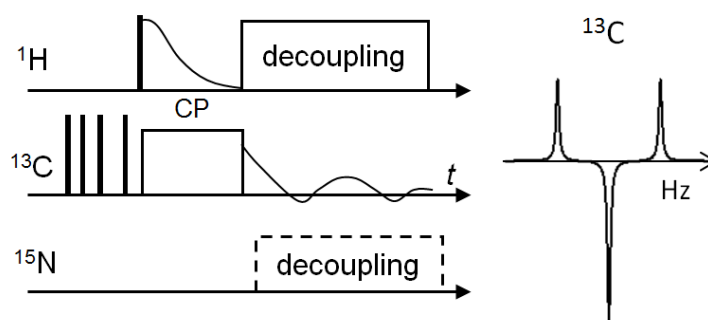


Figure S5a. ^{13}C CP spectra acquired without and with ^{15}N decoupling in alternate scans are subtracted from each other.^{11,12} In the resulting difference spectrum, the central peak of uncoupled spins is suppressed while the signal of ^{13}C - ^{15}N coupled pairs is preserved. A dipolar interaction with abundant ^1H spins is removed by proton decoupling applied to both spectra. In the scans acquired without nitrogen decoupling, the ^{13}C - ^{15}N coupled pairs lead to dipolar doublets in the ^{13}C spectrum, whereas they contribute to a residual central peak in the scans with ^{15}N decoupling. The difference spectrum thus represents a superposition of the ^{13}C - ^{15}N doublet and the central peak of the opposite sign.

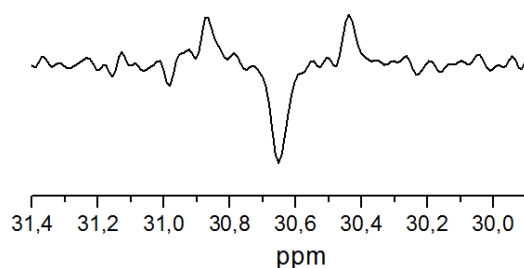


Figure S5b. ^{13}C - ^{15}N dipolar spectrum acquired by recording ^{13}C difference spectra with nitrogen-15 decoupling in alternating scans. 8k scans were accumulated with a relaxation delay of 4 s (12 h measurement time).

S6. Natural abundance deuterium (NAD) NMR

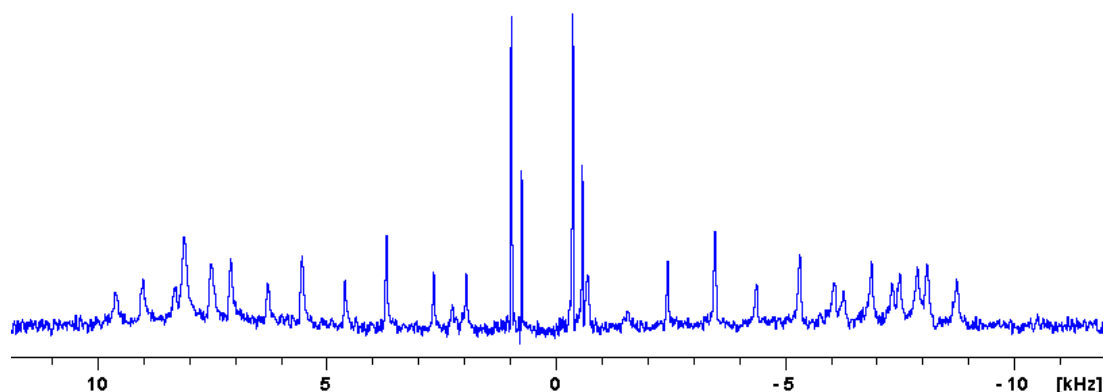


Figure S6. ^2H NMR spectrum of $\text{C}_{12}\text{mimCl}$ in smectic A phase at $110\text{ }^\circ\text{C}$. Spectrum is measured at the natural isotopic abundance of ^2H (0.015%) and in the presence of ^1H decoupling. 128k scans were accumulated with relaxation delay 0.5s (18 h experimental time).

S7. Bond order parameters S_{CH} in the imidazolium ring of the $C_{12}mim$ cation with different anions.

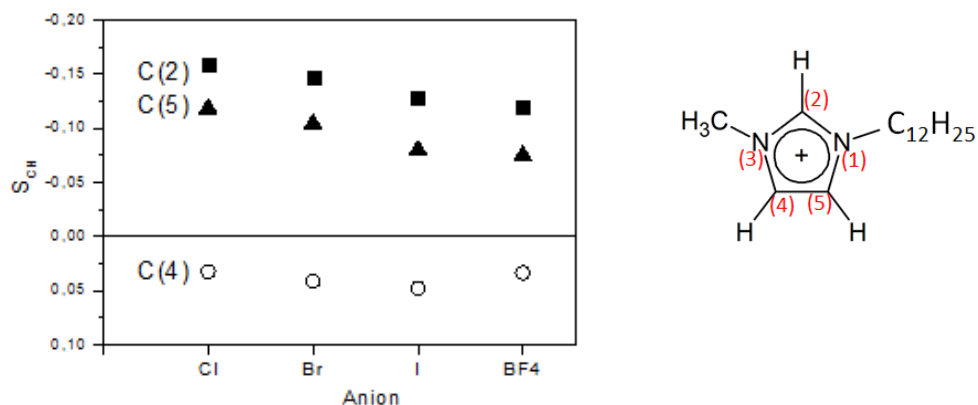


Figure S7. Bond order parameters S_{CH} in the imidazolium ring for the anhydrous $C_{12}mimX$ salts with different anions $X = BF_4, I, Cl,$ and Br . Data are compared at approximately the same difference temperature ΔT with respect to clearing temperature $\Delta T = T - T_C \approx 20^\circ C$.

S8. 1H isotropic chemical shifts

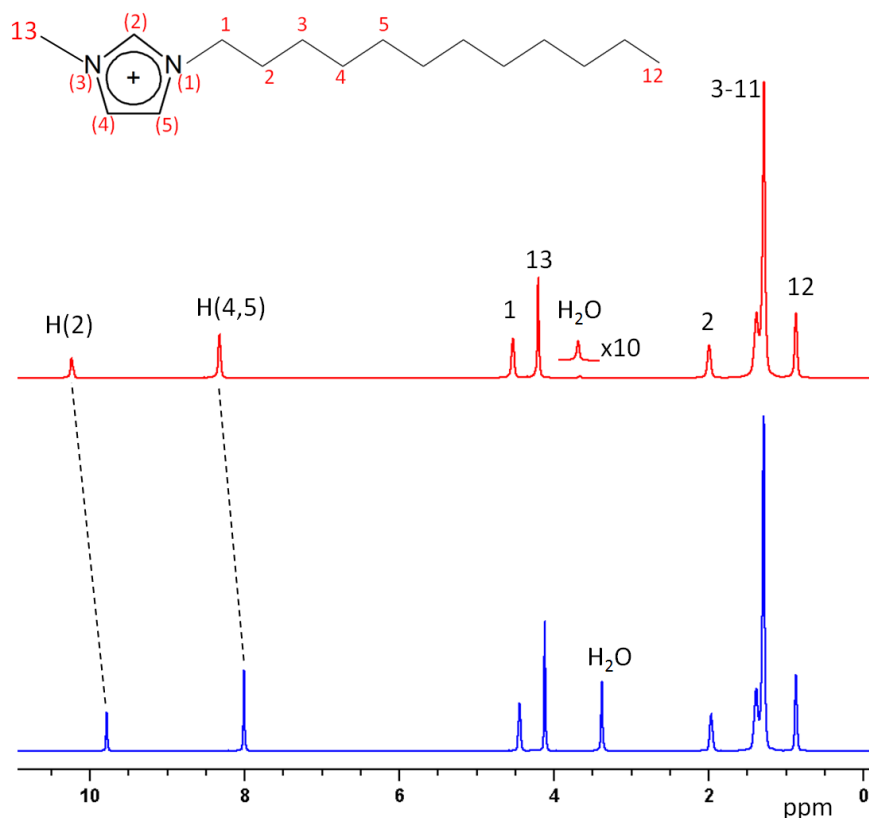


Figure S8. 1H chemical shift spectra of anhydrous (top) and monohydrated $C_{12}mimBr$ (bottom) samples in the isotropic phase.

S9. Water translational diffusion in C₁₂mimBr·H₂O

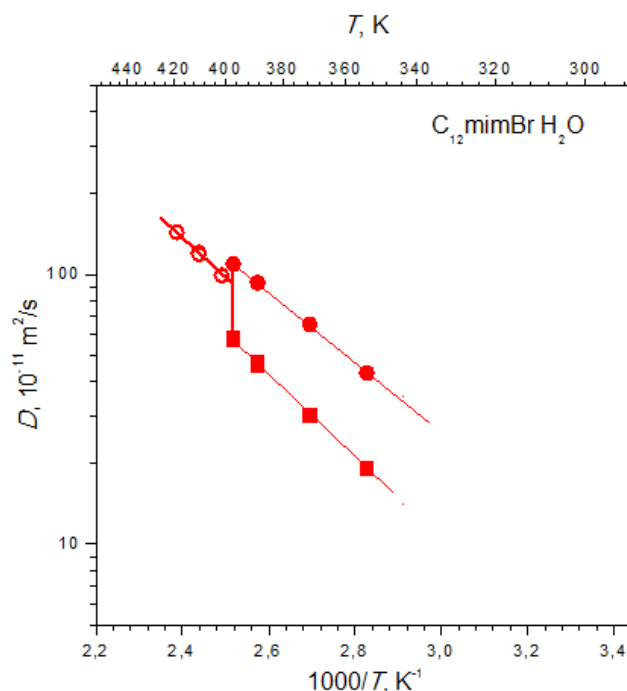


Figure S9. Water diffusion coefficients, D_{iso} (o), D_{\parallel} (■), and D_{\perp} (●) in the isotropic and smectic A phases of C₁₂mimBr·H₂O ionic liquid. Lines are guides for the eye.

References

- 1 S. V. Dvinskikh, in *Modern Methods in Solid-State NMR: A practitioners' Guide*, ed. P. Hodgkinson, Royal Society of Chemistry, Abingdon, 2018.
- 2 B. M. Fung, K. Ermolaev and Y. Yu, *J. Magn. Reson.*, 1999, **138**, 28-35.
- 3 D. P. Burum, M. Linder and R. R. Ernst, *J. Magn. Reson.*, 1981, **44**, 173-188.
- 4 A. E. Bennett, C. M. Rienstra, M. Auger, K. V. Lakshmi and R. G. Griffin, *J. Chem. Phys.*, 1995, **103**, 6951-6958.
- 5 S. V. Dvinskikh, V. Castro and D. Sandström, *Phys. Chem. Chem. Phys.*, 2005, **7**, 3255-3257.
- 6 S. V. Dvinskikh and V. I. Chizhik, *J. Exp. Theor. Phys.*, 2006, **102**, 91-101.
- 7 S. Berger and S. Braun, *200 and More NMR Experiments: A Practical Course*, Wiley, Leipzig, 2004.
- 8 J. S. Lee and A. K. Khitritin, *J. Chem. Phys.*, 2008, **128**, 114504.
- 9 D. Sandström and M. H. Levitt, *J. Am. Chem. Soc.*, 1996, **118**, 6966-6974.
- 10 L. B. Krivdin and E. W. Della, *Progr. Nucl. Magn. Reson. Spectrosc.*, 1991, **23**, 301-610.
- 11 L. Jackalin, B. B. Kharkov, A. V. Komolkin and S. V. Dvinskikh, *Phys. Chem. Chem. Phys.*, 2018, **20**, 22187-22196.
- 12 M. Cifelli, V. Domenici, V. I. Chizhik and S. V. Dvinskikh, *Appl. Magn. Reson.*, 2018, **4**, 553-562.